Biochemistry
Cite This: Biochemistry 2018, 57, 3995−4004
Perspective
pubs.acs.org/biochemistry

Tissue-like Neural Probes for Understanding and Modulating the Brain

Guosong Hong,[†] Robert D. Viveros,[‡] Theodore J. Zwang,[†] Xiao Yang,[†] and Charles M. Lieber*[,†,‡]

[†]Department of Chemistry and Chemical Biology, Harvard University, Cambridge, Massachusetts 02138, United States
[‡]John A. Paulson School of Engineering and Applied Sciences, Harvard University, Cambridge, Massachusetts 02138, United States

ABSTRACT: Electrophysiology tools have contributed substantially to understanding brain function, yet the capabilities of conventional electrophysiology probes have remained limited in key ways because of large structural and mechanical mismatches with respect to neural tissue. In this Perspective, we discuss how the general goal of probe design in biochemistry, that the probe or label have a minimal impact on the properties and function of the system being studied, can be realized by minimizing structural, mechanical, and topological differences between neural probes and brain tissue, thus leading to a new paradigm of tissue-like mesh electronics. The unique properties and capabilities of the tissue-like mesh electronics as well as future opportunities are summarized. First, we discuss the design of an ultraflexible and open mesh structure of electronics that is tissue-like and can be delivered in the brain via minimally invasive syringe injection like molecular and macromolecular pharmaceuticals. Second, we describe the unprecedented tissue healing without chronic immune response that leads to seamless three-dimensional integration with a natural distribution of neurons and other key cells through these tissue-like probes. These unique characteristics lead to unmatched stable long-term, multiplexed mapping and modulation of neural circuits at the single-neuron level on a year time scale. Last, we offer insights on several exciting future directions for the tissue-like electronics paradigm that capitalize on their unique properties to explore biochemical interactions and signaling in a "natural" brain environment.

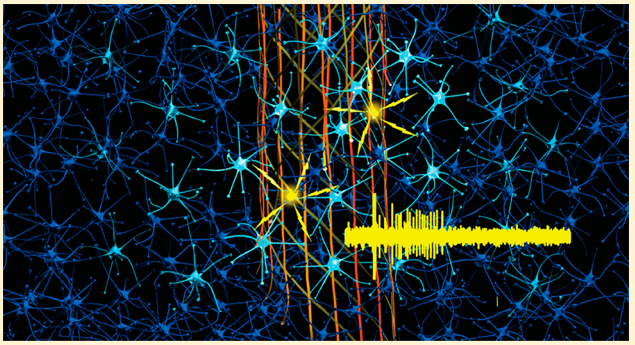

Tools that can provide spatially resolved, real time, and quantitative measures of the electrical activity of neurons are crucial to understanding the brain.[1] Since a capillary electrometer by Adrian[2] and a cathode ray oscilloscope by Erlanger and Gasser[3] were used for recording electrical signals conducted by nerve fibers, scientists have strived to develop tools that can improve the understanding of both the basic electrophysiology of single neurons and the functional connectivity of many neurons in the entire brain.[4,5] Despite advancements over the past century, substantial limitations of electrophysiology probes have remained due to their fundamental structural, mechanical, and topological differences with respect to neural tissue they are designed to interrogate; that is, these differences cause conventional probes to disrupt the natural properties and function of the system being studied. Recognizing this issue, one can ask what structural, mechanical, topological, and ultimately biochemical properties would define an ideal electrophysiology probe.

From a structural perspective, the brain features a large variety of components with sizes ranging from tens of nanometers for synapses that connect individual neurons to tens of centimeters for long-range projections that connect distinct brain regions.[1] In comparison, silicon microelectrode arrays have overall probe sizes that are always >4 times larger than a single neuron,[6,7] although subcellular-sized recording electrodes with high density and multiplexity can be achieved by top-down fabrication processes.[8] On the other hand, microwire-based brain probes become significantly larger than neuron somata with an increase in the number of channels,[9] despite the subcellular feature size for single-channel carbon electrodes.[10,11] The relatively large size of probes may disrupt the natural three-dimensional (3D) neural connectivity and activity of relatively dense neural tissue comprising interconnected neurons, glial cells, and blood vessels at the implanted site and lead to an unfavorable chronic immune response.

From a mechanical perspective, conventional brain probes also differ significantly from brain tissue. Brain tissue is extremely soft, with a small Young's modulus of 0.1−16 kPa and a bending stiffness of 10^{-4} to 10^{-1} nN m per unit width for a 20−100 μm thick brain slice.[12,13] In striking contrast, the bending stiffness values for typical 15 μm thick Si probes, $\sim 10^5$ nN m,[14,15] single-channel carbon electrodes with diameters of <10 μm, $\sim 10^4$ nN m,[10,15] and typical "flexible" probes fabricated on 10−20 μm thick bendable polyimide substrates, 10^3−10^4 nN m,[16] are at least 100000−1000000 times greater

Special Issue: Molecules and the Brain

Received: February 1, 2018
Revised: March 8, 2018
Published: March 12, 2018

DOI: 10.1021/acs.biochem.8b00122
Biochemistry 2018, 57, 3995−4004

than that of the tissue they are designed to interrogate. The high rigidity of these common probes is primarily due to the large Young's moduli, which describe the inability of materials to deform, and the thickness of the materials used in their construction. Importantly, this large mismatch in bending stiffness leads to relative shear motion between brain tissue and the neural probes and evokes a chronic immune response that produces glial scar formation and neuron depletion at probe–brain interfaces.[17] The near universal chronic immune response is believed to be the main contributor to the reported degradation of recording and stimulation capabilities over extended time periods with common probes.[18]

From a topological perspective, the brain is comprised of highly organized and interconnected 3D networks of neurons and non-neuronal cells, such as astrocytes and microglia, that brain probes should ideally leave intact. There are several characteristics of probe design one should consider to accomplish this. On a local scale, inspired by the high degree of interpenetration between the networks of neurons and glial cells in 3D,[19] the probe should be designed to afford a similar degree of interpenetration between the implanted electronic network and the endogenous neuronal and glial networks by leaving sufficient open space for interpenetration to occur in a 3D topology. On a global scale, via recognition of the cooperative importance of glial cells in defining the functional connectivity and evolution of neuronal networks in the brain,[20,21] the probe design should ensure the absence or at worst a minimal disturbance of the endogenous distribution of neurons and other cells. Despite these design principles of an ideal neural probe, conventional probes necessarily exclude a solid volume of neural tissue permanently, thus not only prohibiting 3D interpenetration with the neuronal and glial networks but also disrupting the endogenous distribution of cells[17] and 3D diffusion of important molecular and macromolecular signaling species.[22]

As a consequence of the aforementioned structural, mechanical, and topological mismatches between neural tissue and the electronic probes designed to study the neural tissue, conventional implantable brain probes adversely impact the properties and function of the neural systems being studied and are thus generally incapable of achieving a chronically stable interface with the endogenous neural network and affording consistent long-term monitoring and modulation of brain activity at the single-neuron level.[23−28] Thus, we have focused on fundamentally new probe concepts that overcome these limitations by eliminating the distinction between the neural and electronic systems with "tissue-like" neural probes.[15,29−35]

MESH ELECTRONICS IS DESIGNED TO MIMIC NEURAL TISSUE

Early on we began to focus on this goal of merging electronic and neural systems by developing subcellular-sized nanowire field-effect transistor (FET) detectors[36−38] and porous 3D flexible device arrays.[39,40] The small sizes of nanowire FETs without loss of measurement sensitivity have allowed them to probe cells in a highly localized manner,[41,42] allowing the formation of artificial synapses with neurites[37] and minimally invasive intracellular recording.[38,43] Incorporation of addressable nanoelectronic devices into a 3D tissue scaffold (macroporous nanoelectronic scaffold) followed by cell seeding and culture also led to the demonstration of electronically innervated synthetic neural and cardiac tissues, where the bidirectional flow of electrical and chemical signals between interpenetrated cellular and electronic networks allows simultaneous monitoring and modulation of network activity.[40,44]

The macroporous nanoelectronic scaffold concept for synthetic or engineered tissues placed us tantalizingly close to the goal of seamless 3D integration of electronic recording and stimulation devices within the brain. In particular, the macroporous nanoelectronics scaffold provided a framework now generalized to an open mesh electronics platform,[40,44] in which it is possible to design and realize neural probes that have (1) structural features of functional devices, conductive interconnects, and support elements on the nanometer to micrometer size scale similar to that of cells in neural tissue, (2) mechanical properties on par with those of the endogenous neural tissue, and, critically, (3) macroporous 3D interconnected structures that allow interpenetration of neurons and other cells without altering their endogenous distribution, as well as diffusion of key signaling molecules in the local milieu.[29]

The free-standing mesh electronics[15,29,33] (Figure 1A, I) consists of an array of recording and/or stimulation electrodes with their positions photolithographically defined at one end to target one or more brain regions (green dots in the solid black box). These electrodes are individually connected to input/output (I/O) pads at the other end of the mesh (red dots) via polymer-passivated metal interconnect wires (red lines in the dashed black box), allowing the electrodes to transmit electrical signals to and receive modulation signals from external recording and stimulation instrumentations, respectively. Structurally, the mesh electronics is designed to have widths of longitudinal (long axis) and transverse (short axis) elements smaller than cell soma. In addition, these longitudinal and transverse elements have submicrometer thicknesses, and unit openings in the mesh are generally at least 2 orders of magnitude larger than the soma. Together, these structural features result in an extremely small bending stiffness of the mesh electronics, 10^{-2} to 10^{-1} nN m, similar to that of brain tissue (10^{-4} to 10^{-1} nN m).[32] The unique structural, mechanical, and topological properties of the mesh electronics not only address and overcome the key limitations of previous electrophysiological probes used for understanding and modulating the brain but also set the stage for much more sophisticated biochemical modifications and functionalization of the mesh surface, which is composed of a biocompatible poly(alkylene-arylene oxide) polymer, as will be discussed in Future Directions and Outlook.

UNIQUE DELIVERY OF MESH ELECTRONICS

As a result of the unique structural, mechanical, and topological design of mesh electronics, the ultraflexible, submicrometer thick mesh structures can be suspended in an aqueous solution much like colloids with apparent light scattering (Figure 1A, II).[15,34] At first glance, this characteristic and unique flexibility of the mesh raises a conundrum for minimally invasive delivery to the brain. Conventional silicon, microwire, and polymer neural probes, which have bending stiffness values significantly larger than that of brain tissue, can be directly inserted into the brain at the cost of long-term inflammatory immune response and chronic recording instability.[23−28] In contrast, a similar direct insertion of the tissue-like mesh electronics is not possible, and placing the mesh probe in a surgical incision would be invasive and cause local trauma. If we were to think outside the box, the ultraflexibility of mesh electronics opens up a simple yet effective solution commonly used in biology and

DOI: 10.1021/acs.biochem.8b00122
Biochemistry 2018, 57, 3995−4004

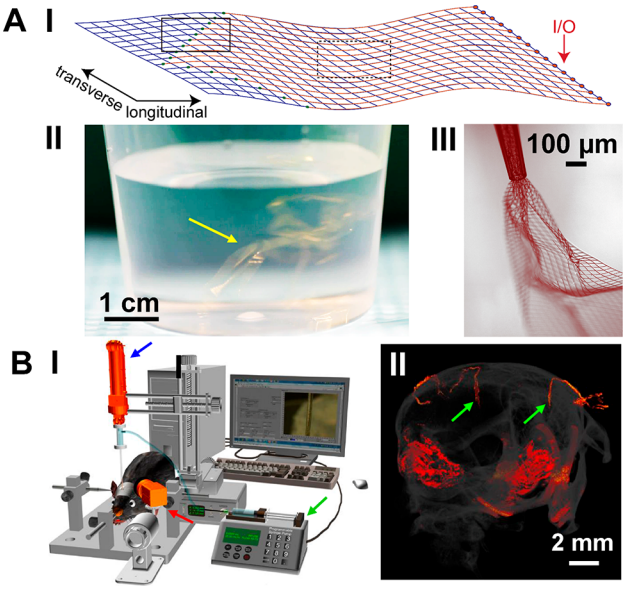

Figure 1. Design and delivery of mesh electronics probes. (A) The unique structural and mechanical design of mesh electronics enables novel syringe-assisted delivery through a needle. (I) Schematic of 16-channel mesh electronics, highlighting the recording electrodes (green dots in the solid black box), metal interconnects (red lines in the dashed black box), and I/O pads (red arrow). (II) Photograph of a beaker with multiple 16-channel mesh electronics probes (yellow arrow) suspended in an aqueous saline solution; the golden color corresponds to light scattered and reflected from 10 μm wide, 100 nm thick metal interconnect lines. (III) Bright-field microscope image taken in wide-field transmission mode showing partially ejected mesh electronics through a glass needle with an inner diameter of 95 μm, exhibiting significant expansion and unfolding of mesh electronics in an aqueous solution. (B) Controlled stereotaxic injection allows precisely targeted delivery of mesh electronics in the brain. (I) Schematic of the semiautomated instrumentation for controlled injection of mesh electronics, highlighting a syringe pump for controlling the volumetric injection rate (green arrow), the motorized translation stage for controlling needle withdrawal (blue arrow), and the CCD camera for visualizing the mesh in the FoV (red arrow). (II) Micro-CT image showing two fully extended mesh electronics probes (red linear structures highlighted by green arrows) within the brain following controlled injection. The other reddish areas correspond to the skull and mesh probe (I/O region) on the outer surface of the skull. Reproduced with permission from refs 15 and 34. Copyright 2015 Macmillan Publishers Limited and American Chemical Society, respectively.

medicine for delivery of species ranging in size from biomolecules to viruses and cells: direct syringe injection through a needle.

A single mesh electronics probe suspended in an aqueous solution can be drawn and loaded into a syringe needle, such as a glass capillary, and then injected under positive pressure into virtually any brain region or other soft tissue in the body like pharmaceuticals and biologics with minimal invasiveness. The first demonstration of the injectable mesh electronics concept by Liu et al. in 2015 showed that centimeter-scale macroporous mesh electronics could be injected through needles with inner diameters of <100 μm (Figure 1A, III) without damage to the mesh electronics.[15] During injection into a cavity, solution, or bodily fluid, the mesh electronics unrolls and expands from the point of the needle constriction, although it maintains a roughly cylindrical structure when injected into dense tissue. This initial work also led to an indication of the special chronic stability of the mesh electronics injected into neural tissue, but it was limited in terms of the ability to target precisely different brain regions. For example, because the mesh electronics is so flexible, it was subject to crumpling during injection, yielding poorly defined sensor device positions with respect to specific regions within the brain. Specifically, the small size of key subfields and layers of a mouse brain requires precise injection of the mesh probe to ensure targeted delivery to a desired region: for example, the CA1 subfield of the hippocampus is ~620 μm thick, the CA3 subfield is ~230 μm thick,[45] cortical layer V is ~300 μm thick,[46] and the dentate gyrus granular cell layer is ~60 μm thick.[47]

Hong et al. solved this key challenge by developing a semiautomated controlled injection method in which the rates of mesh electronics injection and needle withdrawal are balanced using a standard stereotaxic surgery stage with addition of a motorized translator and charge-coupled device (CCD) imager (Figure 1B, I).[34] The balanced mesh injection/needle retraction is achieved by real time optical tracking of the upper I/O pads of the mesh electronics, which are always outside of the skull, in the field of view (FoV) of the CCD (red arrow, Figure 1B, I). In this manner, it is ensured that the mesh position remains stationary in the FoV during injection by the syringe pump (green arrow, Figure 1B, I) while the needle is moved upward by a computer-controlled linear translation stage (blue arrow, Figure 1B, I). The ability to implant mesh electronics with fully extended structures in targeted brain regions using this methodology was confirmed by micro-computed tomography (micro-CT, Figure 1B, II) and histology.[34] The positioning precision of electrodes in the mesh electronics during the injection process is measured as ~20 μm, smaller than the thickness of key subfields and layers within the brain (~60−600 μm, as noted above[45−47]), and thus indicates that the FoV injection method can achieve precise targeted delivery of mesh electronics. In addition, the common use and availability of stereotaxic injection in neuroscience animal research make this method of delivery straightforward and simple to adopt in other laboratories.

UNIQUE CHRONIC INTERFACE WITH BRAIN TISSUE

Several studies have now demonstrated that the tissue-like properties of mesh electronics yield little or no adverse chronic brain tissue response following injection/implantation of the mesh probes.[30,33] Immunohistological staining of brain tissue after implantation of common silicon,[17] tungsten,[48] and carbon[10] brain probes has established that these probes evoke chronic immune responses at the probe−tissue interface as evidenced by neuron depletion and glial scar formation. Studies indicate that the deleterious chronic immune response is in part due to the mechanical mismatch between the neural tissue and the probe, and together, these factors prohibit stable recording and tracking of electrophysiological activities from single neurons over extended time periods.[18,23,28,49−53]

In direct contrast, time-dependent immunohistological studies of brain tissue containing implanted tissue-like mesh electronics have demonstrated tissue healing without evidence for a chronic immune response (Figure 2).[15,30,33,35] Confocal fluorescence images of probe-containing brain slices at 2 weeks, 4 weeks, and 3 months (Figure 2A−C, respectively) revealed several unique features. First, the mesh electronics produced little inflammation at short times (2 weeks) post-implantation, evidenced by an only slight accumulation of astrocytes and

DOI: 10.1021/acs.biochem.8b00122
Biochemistry 2018, 57, 3995−4004

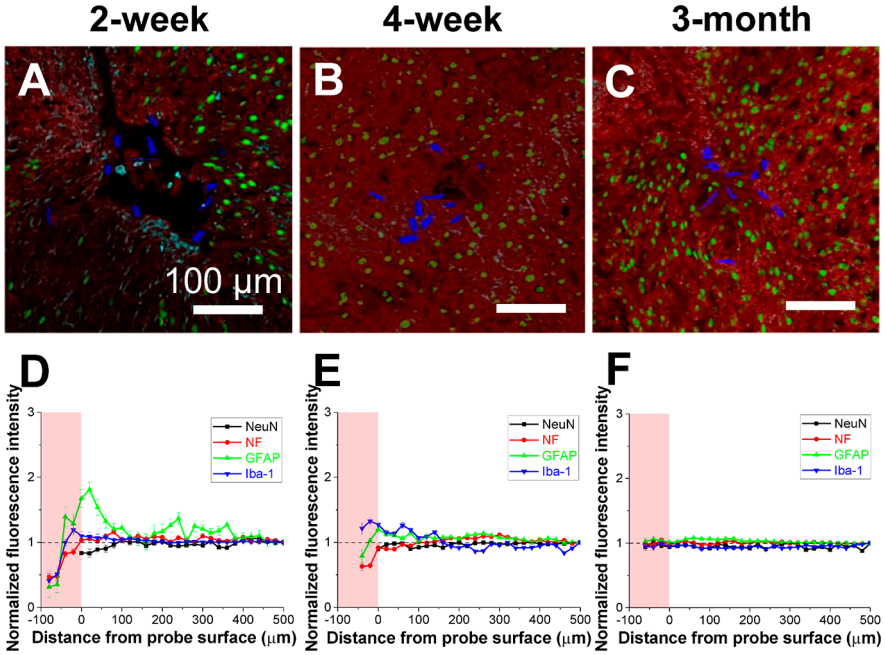

Figure 2. Time-dependent histology of the mesh electronics–brain tissue interface. (A–C) Confocal fluorescence microscopy images of 10 μm thick horizontal brain slices sectioned perpendicular to the long axis of mesh probes at 2, 4, and 12 weeks post-injection, respectively. Green, red, cyan, and blue colors correspond to neuron nuclei (NeuN antibody), neuron axons (neurofilament antibody), astrocytes (glial fibrillary acidic protein, GFAP antibody), and mesh electronics, respectively. (D–F) Normalized fluorescence intensity plotted as a function of distance from the boundary of mesh electronics at 2, 4, and 12 weeks post-injection, respectively. The pink shaded regions indicate the interior of the mesh electronics, and the error bars represent the standard error of the mean (SEM). Reproduced with permission from ref 30. Copyright 2017 National Academy of Sciences.

microglia signals near the mesh boundary, while there was essentially no evidence for a chronic immune response at longer times. Second, images showed that axons and neuron somata started penetrating into the interior of the open mesh electronics at the earliest 2 week time point, and that by 3 months post-injection, there was seamless integration of implanted electronic network and tissue. Third, quantitative immunohistology analyses demonstrated that neuron axons and somata, as well as non-neuronal cells such as astrocytes and microglia, exhibited endogenous distributions from inside to far from the mesh probe (Figure 2D–F). Taken together, these results have shown that, by addressing key structural, mechanical, and topological constraints with our tissue-like mesh electronics, we have been able to realize a probe that minimizes perturbation of the brain tissue we seek to study, in contrast to the case with commonly used electrophysiology tools. This not only has allowed unique measurements that will be described in the following sections but also opens up the unique opportunity to exploit biochemical functionalization of mesh electronics for modulating interactions within the brain, as will be discussed at the end of this Perspective.

MESH ELECTRONICS STABLY MONITORS BRAIN ACTIVITY AT THE SINGLE-NEURON LEVEL

The stable and seamless chronic integration of axons and neuron somata throughout the implanted mesh electronics probes has enabled stable measurements of neural activity without an influence from chronic gliosis present with other probes. In general, information processing in the brain is performed by transduction of electrical signals within neurons and transport of neurotransmitters between neurons. Rapid intracellular depolarization and axonal propagation of the action potential in the presynaptic neurons result in vesicle-mediated release of neurotransmitters, such as dopamine or γ-amino-butyric acid (GABA), which reach the postsynaptic neuron by diffusion across the synaptic cleft. This then elicits a functional response in the postsynaptic neuron and allows for downstream signal propagation.[1] Electrophysiology of neurons manifests from continuous interrogation of changes in intracellular or local extracellular potentials, which occur as a direct result of these electrical and chemical signals.[54] Because of the technical challenges of *in vivo* intracellular patch clamp that is applicable to only acute recordings in anesthetized animals,[55,56] most intracerebral electrophysiology studies employ single-neuron level extracellular monitoring of neuronal activity with a focus on improving chronic stability[33] and increasing the throughput of simultaneously measured neurons.[7,32]

A critical challenge for multiplexed *in vivo* brain mapping with mesh electronics has centered on creating structures that can be readily connected to and disconnected from measurement electronics. It is important that the I/O pads corresponding to each electrode remain separate when being connected to an external recording interface; otherwise, the crossed wires may short circuit and confound data collection. However, the syringe injection process makes it topologically difficult to achieve prebonding of I/O pads to a connector. We first solved this challenge with an automated conductive ink printing method[34] and, subsequently, with a more user-friendly plug-and-play I/O interface.[31] The plug-and-play interface, which allows for direct clamping of the mesh electronics I/O pads into a standard zero-insertion force (ZIF) connector, was implemented by redesigning the region of the mesh external to the skull. The recording region of the mesh probe is kept identical to previous designs (Figure 3A, green inset) to maintain its tissue-like properties, while the external region consists of a leaf-like stem with parallel interconnects

DOI: 10.1021/acs.biochem.8b00122
Biochemistry 2018, 57, 3995–4004

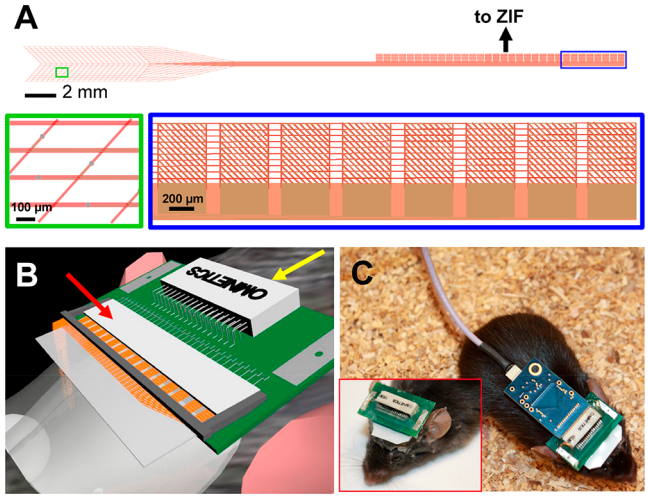

Figure 3. Syringe-injectable mesh electronics with a plug-and-play interface. (A) Schematic diagram of the plug-and-play mesh electronics, where the ultraflexible recording region (green box; bottom left inset, zoom) converges to a flexible stem terminating in mesh metal I/O pads perpendicular to the stem (blue box; bottom right inset, zoom). The stem and mesh I/O remain outside the skull. (B) Schematic diagram of direct clamping of the mesh I/O pads into a PCB-mounted ZIF connector (red arrow), which can then be connected to measurement electronics via a standard Omnetics connector (yellow arrow) mounted on the same PCB. (C) Photograph showing electrophysiological recording of a freely moving mouse injected with mesh electronics. The inset shows the part of the interface that remains permanently attached to the mouse head without the amplifier and the cable connected. Reproduced with permission from refs 29 and 31. Copyright 2018 Elsevier and 2017 American Chemical Society, respectively.

terminating in an array of perpendicularly oriented I/O pads (Figure 3A, blue inset). The width and pitch of the I/O pad array were designed to ensure 100% channel connectivity with blind insertion into the ZIF connector.[31] The external region with I/O pads is injected onto a thin polymer film that allows direct "by-hand" insertion and clamping of the I/O pads into a ZIF connector premounted on a printed circuit board (PCB) (Figure 3B). The PCB is fixed onto the animal's skull as a compact and low-mass interface (1.3 and 0.65 g, with and without the detachable amplifier connected, respectively,[32] compared to at least 3 g for Michigan array silicon probes[7,57]) for removable attachment of measurement electronics during chronic recording from awake restrained or free-moving animals (Figure 3C). In addition to facilitating adoption of the mesh electronics by non-expert laboratories, the plug-and-play interface has also enabled implementation of sterilization protocols necessary for human surgical environments.

Representative chronic recording data from a 32-channel channel mesh probe highlight several key points about measurements with mesh electronics in live rodent brains. First, as demonstrated in previous immunohistology studies, the implanted mesh electronics probe allows the recording electrodes to detect extracellular action potential firing from an endogenous distribution of neurons in the vicinity of the probe (Figure 4A, I). Second, the recorded traces from the 32 recording electrodes that are distributed at different locations spanning the motor cortex exhibit distinct firing patterns (Figure 4A, II, left) with clear firing events represented by "spikes", or extracellular action potential waveforms in the magnified time traces (Figure 4A, II, right). Because the appearance of each spike indicates the firing event from a single neuron, such recordings are usually also termed "single-neuron" or "single-unit" recordings. Third, it is possible for spikes from multiple neurons to be detected simultaneously by the same electrode; however, spikes with origins from different neurons usually display and can be resolved by their distinct waveforms due to differences in relative locations and distances from the same recording electrode.[54] This fact brings immense advantages to processing the single-unit recording data, as it becomes much more computationally efficient to extract all spikes by standard spike sorting algorithms and perform principal component analysis (PCA) to cluster spikes and assign them to different putative neurons based on the differences in waveform. An overlay of sorted and clustered spikes for eight representative channels from the 32-channel multiplexed recordings demonstrates the detection of one or two neurons per electrode (Figure 4A, III).

Using the same approach to process the single-unit recording data, chronic recordings obtained from four separate 32-channel mesh probes implanted into the motor cortex and hippocampus in the right and left hemispheres of a mouse at 2 and 4 months post-injection (Figure 4B) highlight the unique stability and capabilities of tissue-like mesh electronics.[32] For example, single-unit firing activity was detected in roughly 85% of the 128 channels, and the detected activity in each channel generally remained consistent over the 4 month period of the measurements. For example, ~80% of all channels with recorded spikes showed a <20% variation in average spike amplitude, and >90% of detected single units at 2 months remained detectable with aforementioned small changes in amplitude at 4 months. These results contrast with data reported from conventional microwire electrodes[58] and silicon-based Utah array probes,[25] where the majority of channels exhibit a >50% variation in spike amplitude and loss of more than half of initially detected single units only 1 month post-implantation. Thus, the tissue-like mesh electronics provides a substantial advance in capabilities for highly stable and scalable multiplexed chronic recording from the single-neuron level upward.

Highly stable and multiplexed recording probes will be critical for elucidating mechanisms of neural circuit evolution over time spans ranging from months to years important in, for example, natural and pathological aging.[59] Indeed, we have carried out recording studies with implanted mesh electronics over a time scale of nearly a year and showed the capability to stably track and record from the same individual neurons for the first time (Figure 4C).[33] For example, PCA of single-unit activity from individual channels (Figure 4C, I) and firing rate analyses from PCA-identified individual neurons (Figure 4C, II) demonstrated stable neuron spiking waveforms and intrinsic biophysical properties (i.e., action potential firing rates)[60] over an 8 month period without behavioral training. Interestingly, by extension of these studies past 48 weeks, the time at which aging-related changes are observed in mice, chronic recordings with mesh electronics revealed distinct changes in individual neurons (Figure 4C, III). Because no observable changes were found in electrode impedance or cell populations at the mesh probe surface, the neuron-dependent decrease in firing rate can be attributed to biologically intrinsic changes in neuronal and neural circuit properties during aging. The unique capability of mesh electronics to stably monitor brain activity at the single-neuron level over months to years opens up unprecedented opportunities for high-resolution, longitudinal studies to

DOI: 10.1021/acs.biochem.8b00122
Biochemistry 2018, 57, 3995−4004

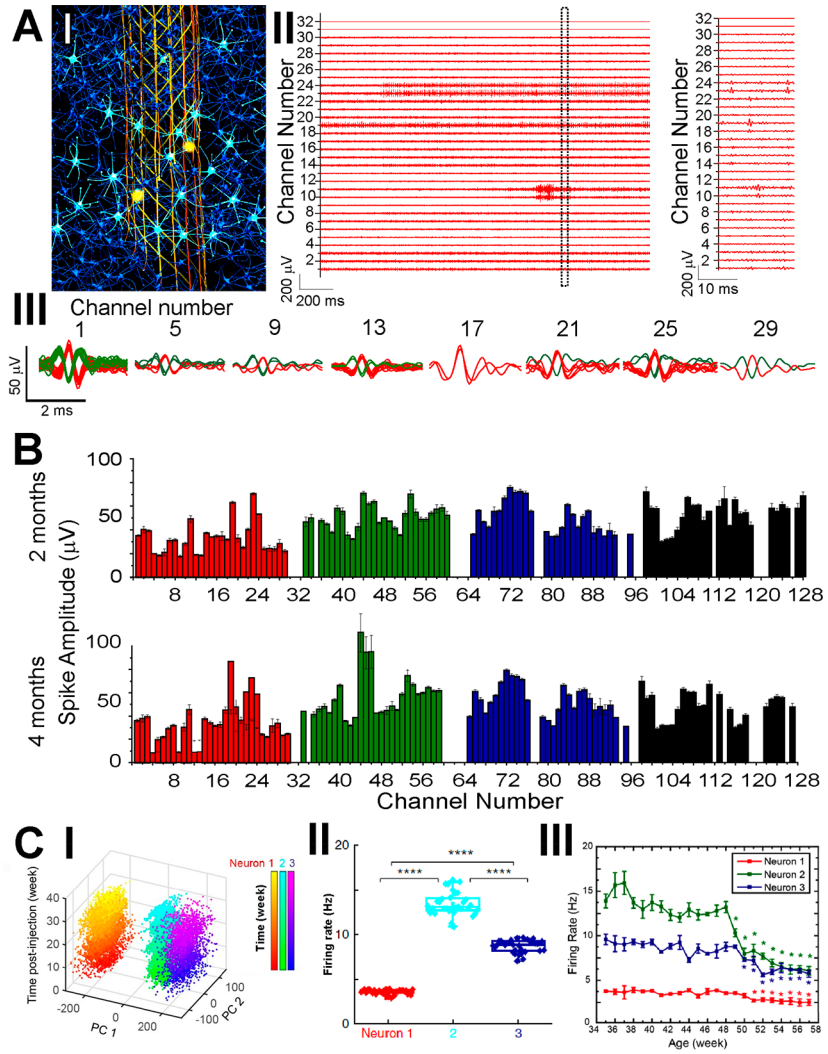

Figure 4. Highly multiplexed, chronically stable *in vivo* electrophysiology in mice. (A) Electrophysiological recording of single-neuron action potentials in mouse brain. (I) Schematic of *in vivo* recording of neuron activities via the seamless integrated interface between the injected mesh electronics and the endogenous neural tissue. Electrically active neurons are colored bright cyan, with their firing activities detected by a subset of recording electrodes (yellow circles) in the mesh electronics at a time. (II) Representative multiplexed extracellular single-neuron recording traces from a 32-channel mesh electronics probe at 2 months post-injection into the mouse motor cortex, with a magnified view of a 20 ms segment highlighting the waveforms of detected single-unit action potentials in channels 10, 11, 19, 23, and 24. (III) Overlay of sorted and clustered spikes from a subset of selected channels by processing the raw data of recording traces shown in part II of panel A. Red and green colors are used to denote spikes assigned to different neurons. (B) Average single-unit spike amplitudes from simultaneous 128-channel recording in a mouse brain using four separate 32-channel mesh electronics probes at 2 and 4 months post-injection. The error bars represent the SEM. (C) Time-dependent consistent tracking of the same individual neurons based on single-unit spike recording, sorting, and clustering as shown in panel A. (I) PCA-separated clusters of single-unit firing activity are stable over the course of 34 weeks post-injection in young mice. (II) PCA-identified neurons from part I of panel C demonstrate stable firing rates across the analyzed 34 weeks. (III) Age-dependent individual neuron firing rate changes in middle-aged mice demonstrate systematic decline. Reproduced with permission from refs 32 and 33. Copyright 2017 National Academy of Sciences and 2016 Macmillan Publishers Limited, respectively.

interrogate age-dependent neural circuit evolution underlying neurodegenerative processes, such as the memory decline and learning impairment associated with Alzheimer's disease, from a single-neuron perspective.

MESH ELECTRONICS CHRONICALLY MODULATES BRAIN ACTIVITY WITH STABLE SINGLE-NEURON RESPONSES

Electrophysiology probes can also be used to modulate brain activity by injection of charge above a threshold determined by neuromodulatory efficacy for stimulation or inhibition of activity.[18,61] While direct electrical modulation serves as the basis for research and therapeutic devices, such as deep brain stimulators used to treat Parkinson's disease,[62,63] the issue of mismatches in structural and physical properties that lead to glial scar formation and micromotion discussed above also limits the stability of research probes and medical implants.[64]

In this context, implantation of tissue-like mesh electronics incorporating both stimulation and recording electrodes into brains (Figure 5A) allows for single-neuron level modulation and recording in a natural tissue environment. Simultaneous stimulation and recording studies showed significantly increased firing rates from neurons adjacent to stimulation electrodes as evidenced by reproducible evoked spike trains in repeated stimulation trials (Figure 5B). Moreover, consistent

DOI: 10.1021/acs.biochem.8b00122
Biochemistry 2018, 57, 3995−4004

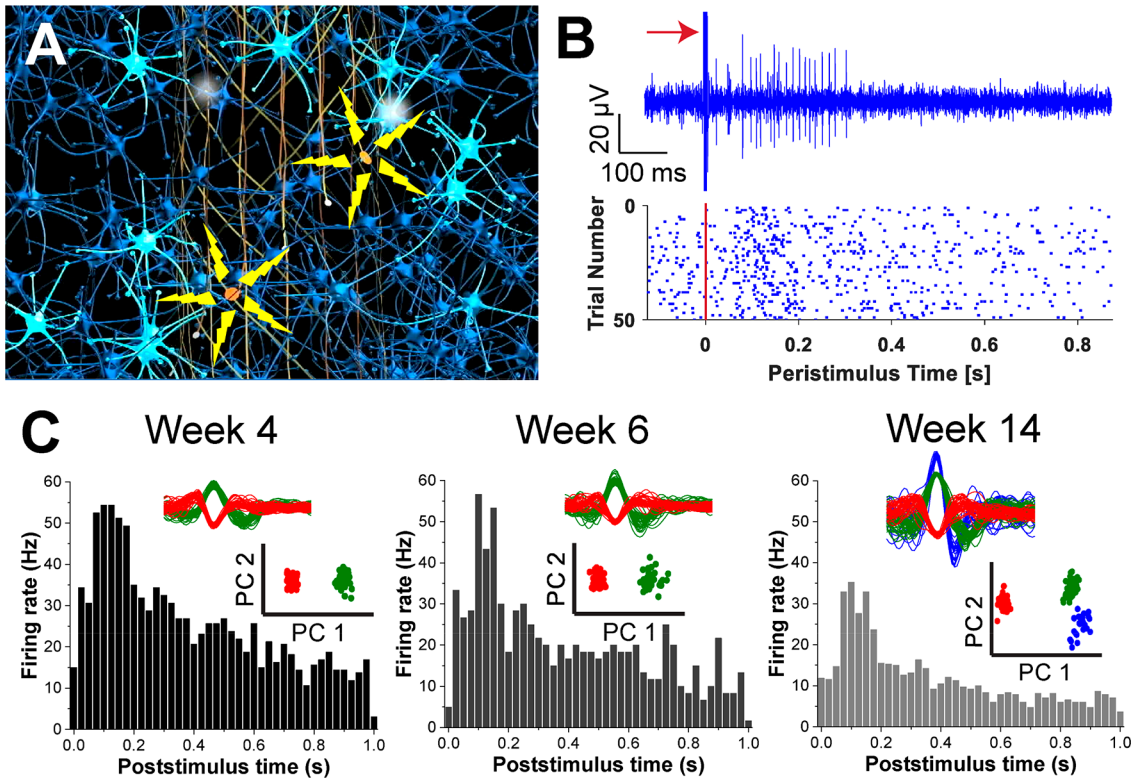

Figure 5. Precision modulation of neural activity. (A) Schematic of mesh electronics with stimulation and recording electrodes where precise circuit modulation with simultaneous recording is highlighted from two stimulation sites. (B) Representative stimulus-evoked single-unit firing trace with a red arrow indicating the stimulus (top) and a raster plot showing single-unit firing events (blue dots) before and after an electrical stimulus is given (red solid line; t = 0 s) for 50 trials (bottom). (C) Post-stimulus time histograms from a representative recording electrode in the vicinity of a stimulation electrode 4, 6, and 14 weeks after injection of the mesh probe. Spike sorting and PCA clustering results with corresponding colors for different neurons are shown as insets. Reproduced with permission from ref 33. Copyright 2016 Macmillan Publishers Limited.

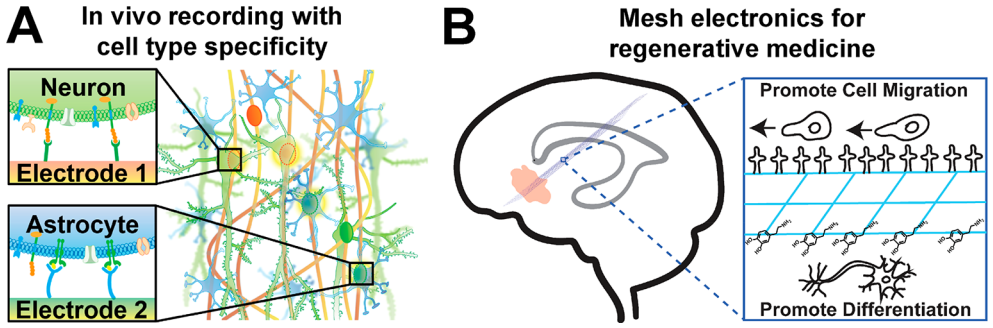

Figure 6. Future directions for tissue-like mesh electronics. (A) Antibodies or aptamers on electrodes could be used to attract and target specific cell types, allowing selective electrophysiological monitoring of different cell types on different electrodes. (B) Mesh electronics (blue) could be used to connect brain regions containing NPCs (gray) to sites of tissue damage (pink). Biochemical modification of the surfaces of mesh electronics could be used to promote cellular migration toward damage and differentiation to desired cell types near damage while monitoring and/or modulating activity with the integrated electrodes.

patterns of post-stimulus firing rate modulation from 4 to 14 weeks post-injection of mesh electronics along with spike sorting and PCA analyses confirmed stable single-neuron responses to chronic electrical stimulation over this time period (Figure 5C). The detection of a new neuron at 14 weeks (blue, Figure 5C), which can be attributed to the long-term changes in the local neural circuits as a result of chronic modulation, represents a unique opportunity for future studies. For example, the demonstrated chronic stability of tissue-like mesh electronics with simultaneous modulation and recording could be used to probe causality in neural networks in the absence of deleterious "probe-induced" cell and tissue changes.

FUTURE DIRECTIONS AND OUTLOOK

The unique characteristics of syringe-injectable mesh electronics as a tissue-like neural probe could enable unprecedented future studies and provide new insight into a variety of biological phenomena in neuroscience and neurology. In particular, many experiments can benefit from the simple, minimally invasive delivery to targeted brain regions, the ability to modify the probe surface with biochemically active molecules, and their long-term biochemical stability that allows them to chronically monitor and modulate electrophysiological and chemical processes in the brain with single-neuron resolution. Below we highlight several general directions for

DOI: 10.1021/acs.biochem.8b00122
Biochemistry 2018, 57, 3995−4004

mesh electronics and how they could be used to probe the endogenous biochemical interactions and signaling in a "natural" brain environment (Figure 6).

The first example we consider comes from recognizing the inability of implanted electrophysiological probes to target and record from specific cell types or neuron subtypes versus the capability to target and optically image or stimulate specific neuron subtype activity using genetically encoded calcium and voltage indicators[65] or optogenetics,[66] respectively. The natural distribution of both neurons and glial cells achieved post-implantation with tissue-like mesh electronics suggests that functionalization of recording and/or stimulation devices with antibodies or aptamers capable of recognizing and targeting specific cell surface receptors could enable *in vivo* neuron subtype electrophysiology (Figure 6A). We believe the development of such capabilities could open up broad new opportunities for electrophysiology tools, such as deconstruction of complex neural circuitry based on selective recording from specific subgroups of neurons. Additionally, this capability could enable more efficacious electrotherapeutic treatment of neurological diseases such as Parkinson's disease. We envisage that functionalized electrodes in mesh electronics could selectively target and stimulate medium spiny neurons (MSNs) expressing dopamine type 1 (D1) receptors versus D2 receptors, which are structurally and functionally intertwined to facilitate and inhibit movements via direct and indirect pathways, respectively.[67] By selective inhibitory stimulation of D2-receptor expressing MSNs in the "motor-inhibiting" indirect pathway, mesh electronics could restore the normal motor functions in Parkinsonian patients with a much lower therapeutic threshold and long-term safety and efficacy.[67,68]

In a similar vein, our previous *in vitro* studies using functionalized nanowire FETs for biochemical sensing[36,69,70] and subcellular-resolution electrophysiological recording[38,43] could open up completely new opportunities for mesh electronics in the future. For example, receptor-functionalized nanowire FETs incorporated into mesh electronics could be used for highly localized, nondestructive detection of neurotransmitters *in vivo*.[41,71,72] Furthermore, nanowire FET devices functionalized with phospholipids[38,43,73] or cell-penetrating peptides[74] could enable *in vivo* intracellular recording of multiple neurons simultaneously. Such technology would open substantial new opportunities for understanding and influencing brain activity by providing a direct intracellular interface in live animals.[72,75−77]

We believe that implanted mesh electronics also holds substantial potential for regenerative medicine. The underlying motivation of this direction builds upon the use of earlier mesh electronics as an "active" engineered neural tissue scaffold[40] and observations that mesh electronics, when injected into the lateral ventricle of a live mouse, acted as a scaffold to guide the migration of neural cells.[15] Our more recent histological studies showing the interpenetration of neuron axons and somata into the interior of mesh electronics days to weeks post-injection[30,33] call for further investigations to elucidate the relative contributions of tissue remodeling, neurite growth, and migration and development of neural progenitor cells (NPCs). Surface modification of mesh electronics with functional biomolecules known to interact with NPCs and facilitate migration[78] or differentiation[79] could be employed to improve the therapeutic capability of mesh electronics (Figure 6B). By understanding and exploiting the extracellular matrix (ECM)-like properties of mesh electronics to favor migration and development of NPCs from the subventricular and subgranular zones,[80] while simultaneously monitoring and possibly modulating neural activity and circuit connectivity, we envision the potential of targeted injection of mesh electronics to connect endogenous sources of NPCs to regions of damaged tissue for neural tissue repair.

AUTHOR INFORMATION

Corresponding Author

*E-mail: cml@cmliris.harvard.edu.

ORCID

Charles M. Lieber: 0000-0002-6660-2456

Funding

This work was funded by the Air Force Office of Scientific Research (FA9550-14-1-0136), a Harvard University Physical Sciences and Engineering Accelerator award, the National Institute on Drug Abuse of the National Institutes of Health (1R21DA043985-01), and a National Institutes of Health Director's Pioneer Award (1DP1EB025835-01). G.H. is supported by the Pathway to Independence Award (Parent K99/R00) from the National Institute on Aging of the National Institutes of Health (1K99AG056636-01).

Notes

The authors declare no competing financial interest.

ACKNOWLEDGMENTS

The authors thank the members of the Lieber lab for helpful discussions.

REFERENCES

(1) Kandel, E. R., Schwartz, J. H., Jessell, T. M., Siegelbaum, S. A., and Hudspeth, A. J. (2013) *Principles of neural science*, McGraw-Hill, New York.

(2) Adrian, E. D. (1928) *The basis of sensation: The action of the sense organs*, Christophers, London.

(3) Gasser, H. S., and Erlanger, J. (1922) A study of the action currents of nerve with the cathode ray oscillograph. *Am. J. Physiol. 62*, 496−524.

(4) Yuste, R. (2015) From the neuron doctrine to neural networks. *Nat. Rev. Neurosci. 16*, 487−497.

(5) Glickstein, M. (2014) *Neuroscience: A historical introduction*, MIT Press, Cambridge, MA.

(6) Berenyi, A., Somogyvari, Z., Nagy, A. J., Roux, L., Long, J. D., Fujisawa, S., Stark, E., Leonardo, A., Harris, T. D., and Buzsaki, G. (2014) Large-scale, high-density (up to 512 channels) recording of local circuits in behaving animals. *J. Neurophysiol. 111*, 1132−1149.

(7) Jun, J. J., Steinmetz, N. A., Siegle, J. H., Denman, D. J., Bauza, M., Barbarits, B., Lee, A. K., Anastassiou, C. A., Andrei, A., Aydin, C., Barbic, M., Blanche, T. J., Bonin, V., Couto, J., Dutta, B., Gratiy, S. L., Gutnisky, D. A., Hausser, M., Karsh, B., Ledochowitsch, P., Lopez, C. M., Mitelut, C., Musa, S., Okun, M., Pachitariu, M., Putzeys, J., Rich, P. D., Rossant, C., Sun, W. L., Svoboda, K., Carandini, M., Harris, K. D., Koch, C., O'Keefe, J., and Harris, T. D. (2017) Fully integrated silicon probes for high-density recording of neural activity. *Nature 551*, 232−236.

(8) Shobe, J. L., Claar, L. D., Parhami, S., Bakhurin, K. I., and Masmanidis, S. C. (2015) Brain activity mapping at multiple scales with silicon microprobes containing 1,024 electrodes. *J. Neurophysiol. 114*, 2043−2052.

(9) Schwarz, D. A., Lebedev, M. A., Hanson, T. L., Dimitrov, D. F., Lehew, G., Meloy, J., Rajangam, S., Subramanian, V., Ifft, P. J., Li, Z., Ramakrishnan, A., Tate, A., Zhuang, K. Z., and Nicolelis, M. A. L. (2014) Chronic, wireless recordings of large-scale brain activity in freely moving rhesus monkeys. *Nat. Methods 11*, 670−676.

DOI: 10.1021/acs.biochem.8b00122
Biochemistry 2018, 57, 3995−4004

(10) Kozai, T. D. Y., Langhals, N. B., Patel, P. R., Deng, X. P., Zhang, H. N., Smith, K. L., Lahann, J., Kotov, N. A., and Kipke, D. R. (2012) Ultrasmall implantable composite microelectrodes with bioactive surfaces for chronic neural interfaces. *Nat. Mater. 11*, 1065−1073.
(11) Guitchounts, G., Markowitz, J. E., Liberti, W. A., and Gardner, T. J. (2013) A carbon-fiber electrode array for long-term neural recording. *J. Neural Eng. 10*, 046016.
(12) Tyler, W. J. (2012) OPINION The mechanobiology of brain function. *Nat. Rev. Neurosci. 13*, 867−878.
(13) Steif, P. S. (2012) *Mechanics of materials*, Pearson, Upper Saddle River, NJ.
(14) Lee, H., Bellamkonda, R. V., Sun, W., and Levenston, M. E. (2005) Biomechanical analysis of silicon microelectrode-induced strain in the brain. *J. Neural Eng. 2*, 81−89.
(15) Liu, J., Fu, T. M., Cheng, Z. G., Hong, G. S., Zhou, T., Jin, L. H., Duvvuri, M., Jiang, Z., Kruskal, P., Xie, C., Suo, Z. G., Fang, Y., and Lieber, C. M. (2015) Syringe-injectable electronics. *Nat. Nanotechnol. 10*, 629−636.
(16) Rousche, P. J., Pellinen, D. S., Pivin, D. P., Williams, J. C., Vetter, R. J., and Kipke, D. R. (2001) Flexible polyimide-based intracortical electrode arrays with bioactive capability. *IEEE Trans. Biomed. Eng. 48*, 361−371.
(17) Biran, R., Martin, D. C., and Tresco, P. A. (2005) Neuronal cell loss accompanies the brain tissue response to chronically implanted silicon microelectrode arrays. *Exp. Neurol. 195*, 115−126.
(18) Chen, R., Canales, A., and Anikeeva, P. (2017) Neural recording and modulation technologies. *Nat. Rev. Mater. 2*, 16093.
(19) Kasthuri, N., Hayworth, K. J., Berger, D. R., Schalek, R. L., Conchello, J. A., Knowles-Barley, S., Lee, D., Vazquez-Reina, A., Kaynig, V., Jones, T. R., Roberts, M., Morgan, J. L., Tapia, J. C., Seung, H. S., Roncal, W. G., Vogelstein, J. T., Burns, R., Sussman, D. L., Priebe, C. E., Pfister, H., and Lichtman, J. W. (2015) Saturated Reconstruction of a Volume of Neocortex. *Cell 162*, 648−661.
(20) Eroglu, C., and Barres, B. A. (2010) Regulation of synaptic connectivity by glia. *Nature 468*, 223−231.
(21) Clarke, L. E., and Barres, B. A. (2013) Emerging roles of astrocytes in neural circuit development. *Nat. Rev. Neurosci. 14*, 311−321.
(22) Saxena, T., and Bellamkonda, R. V. (2015) Implantable electronics: A sensor web for neurons. *Nat. Mater. 14*, 1190−1191.
(23) Polikov, V. S., Tresco, P. A., and Reichert, W. M. (2005) Response of brain tissue to chronically implanted neural electrodes. *J. Neurosci. Methods 148*, 1−18.
(24) Perge, J. A., Homer, M. L., Malik, W. Q., Cash, S., Eskandar, E., Friehs, G., Donoghue, J. P., and Hochberg, L. R. (2013) Intra-day signal instabilities affect decoding performance in an intracortical neural interface system. *J. Neural Eng. 10*, 036004.
(25) Dickey, A. S., Suminski, A., Amit, Y., and Hatsopoulos, N. G. (2009) Single-Unit Stability Using Chronically Implanted Multi-electrode Arrays. *J. Neurophysiol. 102*, 1331−1339.
(26) Jackson, A., and Fetz, E. E. (2007) Compact movable microwire array for long-term chronic unit recording in cerebral cortex of primates. *J. Neurophysiol. 98*, 3109−3118.
(27) Aflalo, T., Kellis, S., Klaes, C., Lee, B., Shi, Y., Pejsa, K., Shanfield, K., Hayes-Jackson, S., Aisen, M., Heck, C., Liu, C., and Andersen, R. A. (2015) Decoding motor imagery from the posterior parietal cortex of a tetraplegic human. *Science 348*, 906−910.
(28) Bensmaia, S. J., and Miller, L. E. (2014) Restoring sensorimotor function through intracortical interfaces: progress and looming challenges. *Nat. Rev. Neurosci. 15*, 313−325.
(29) Hong, G., Yang, X., Zhou, T., and Lieber, C. M. (2018) Mesh electronics: a new paradigm for tissue-like brain probes. *Curr. Opin. Neurobiol. 50*, 33−41.
(30) Zhou, T., Hong, G., Fu, T. M., Yang, X., Schuhmann, T. G., Viveros, R. D., and Lieber, C. M. (2017) Syringe-injectable mesh electronics integrate seamlessly with minimal chronic immune response in the brain. *Proc. Natl. Acad. Sci. U. S. A. 114*, 5894−5899.
(31) Schuhmann, T. G., Yao, J., Hong, G., Fu, T.-M., and Lieber, C. M. (2017) Syringe-Injectable Electronics with a Plug-and-Play Input/Output Interface. *Nano Lett. 17*, 5836−5842.
(32) Fu, T. M., Hong, G., Viveros, R. D., Zhou, T., and Lieber, C. M. (2017) Highly scalable multichannel mesh electronics for stable chronic brain electrophysiology. *Proc. Natl. Acad. Sci. U. S. A. 114*, E10046−E10055.
(33) Fu, T. M., Hong, G. S., Zhou, T., Schuhmann, T. G., Viveros, R. D., and Lieber, C. M. (2016) Stable long-term chronic brain mapping at the single-neuron level. *Nat. Methods 13*, 875−882.
(34) Hong, G. S., Fu, T. M., Zhou, T., Schuhmann, T. G., Huang, J. L., and Lieber, C. M. (2015) Syringe Injectable Electronics: Precise Targeted Delivery with Quantitative Input/Output Connectivity. *Nano Lett. 15*, 6979−6984.
(35) Xie, C., Liu, J., Fu, T. M., Dai, X. C., Zhou, W., and Lieber, C. M. (2015) Three-dimensional macroporous nanoelectronic networks as minimally invasive brain probes. *Nat. Mater. 14*, 1286−1292.
(36) Cui, Y., Wei, Q. Q., Park, H. K., and Lieber, C. M. (2001) Nanowire nanosensors for highly sensitive and selective detection of biological and chemical species. *Science 293*, 1289−1292.
(37) Patolsky, F., Timko, B. P., Yu, G. H., Fang, Y., Greytak, A. B., Zheng, G. F., and Lieber, C. M. (2006) Detection, stimulation, and inhibition of neuronal signals with high-density nanowire transistor arrays. *Science 313*, 1100−1104.
(38) Tian, B. Z., Cohen-Karni, T., Qing, Q., Duan, X. J., Xie, P., and Lieber, C. M. (2010) Three-Dimensional, Flexible Nanoscale Field-Effect Transistors as Localized Bioprobes. *Science 329*, 830−834.
(39) Lieber, C. M. (2007) Nanotechnology and the Life Sciences. Nano/Bio Interface Center (NBIC) Award for Research Excellence in Nanotechnology Speech; University of Pennsylvania, Philadelphia.
(40) Tian, B. Z., Liu, J., Dvir, T., Jin, L. H., Tsui, J. H., Qing, Q., Suo, Z. G., Langer, R., Kohane, D. S., and Lieber, C. M. (2012) Macroporous nanowire nanoelectronic scaffolds for synthetic tissues. *Nat. Mater. 11*, 986−994.
(41) Zhang, A. Q., and Lieber, C. M. (2016) Nano-Bioelectronics. *Chem. Rev. 116*, 215−257.
(42) Tian, B. Z., and Lieber, C. M. (2013) Synthetic Nanoelectronic Probes for Biological Cells and Tissues. *Annu. Rev. Anal. Chem. 6*, 31−51.
(43) Qing, Q., Jiang, Z., Xu, L., Gao, R. X., Mai, L. Q., and Lieber, C. M. (2014) Free-standing kinked nanowire transistor probes for targeted intracellular recording in three dimensions. *Nat. Nanotechnol. 9*, 142−147.
(44) Dai, X. C., Zhou, W., Gao, T., Liu, J., and Lieber, C. M. (2016) Three-dimensional mapping and regulation of action potential propagation in nanoelectronics-innervated tissues. *Nat. Nanotechnol. 11*, 776−782.
(45) Lein, E. S., Hawrylycz, M. J., Ao, N., Ayres, M., Bensinger, A., Bernard, A., Boe, A. F., Boguski, M. S., Brockway, K. S., Byrnes, E. J., Chen, L., Chen, L., Chen, T. M., Chi Chin, M., Chong, J., Crook, B. E., Czaplinska, A., Dang, C. N., Datta, S., Dee, N. R., Desaki, A. L., Desta, T., Diep, E., Dolbeare, T. A., Donelan, M. J., Dong, H. W., Dougherty, J. G., Duncan, B. J., Ebbert, A. J., Eichele, G., Estin, L. K., Faber, C., Facer, B. A., Fields, R., Fischer, S. R., Fliss, T. P., Frensley, C., Gates, S. N., Glattfelder, K. J., Halverson, K. R., Hart, M. R., Hohmann, J. G., Howell, M. P., Jeung, D. P., Johnson, R. A., Karr, P. T., Kawal, R., Kidney, J. M., Knapik, R. H., Kuan, C. L., Lake, J. H., Laramee, A. R., Larsen, K. D., Lau, C., Lemon, T. A., Liang, A. J., Liu, Y., Luong, L. T., Michaels, J., Morgan, J. J., Morgan, R. J., Mortrud, M. T., Mosqueda, N. F., Ng, L. L., Ng, R., Orta, G. J., Overly, C. C., Pak, T. H., Parry, S. E., Pathak, S. D., Pearson, O. C., Puchalski, R. B., Riley, Z. L., Rockett, H. R., Rowland, S. A., Royall, J. J., Ruiz, M. J., Sarno, N. R., Schaffnit, K., Shapovalova, N. V., Sivisay, T., Slaughterbeck, C. R., Smith, S. C., Smith, K. A., Smith, B. I., Sodt, A. J., Stewart, N. N., Stumpf, K. R., Sunkin, S. M., Sutram, M., Tam, A., Teemer, C. D., Thaller, C., Thompson, C. L., Varnam, L. R., Visel, A., Whitlock, R. M., Wohnoutka, P. E., Wolkey, C. K., Wong, V. Y., Wood, M., Yaylaoglu, M. B., Young, R. C., Youngstrom, B. L., Feng Yuan, X., Zhang, B., Zwingman, T. A., and Jones, A. R. (2007) Genome-wide

DOI: 10.1021/acs.biochem.8b00122
Biochemistry 2018, 57, 3995−4004

atlas of gene expression in the adult mouse brain. *Nature 445*, 168−176.
(46) Hattox, A. M., and Nelson, S. B. (2007) Layer V neurons in mouse cortex projecting to different targets have distinct physiological properties. *J. Neurophysiol. 98*, 3330−3340.
(47) Buckmaster, P. S., Wen, X., Toyoda, I., Gulland, F. M., and Van Bonn, W. (2014) Hippocampal neuropathology of domoic acid-induced epilepsy in California sea lions (Zalophus californianus). *J. Comp. Neurol. 522*, 1691−1706.
(48) Prasad, A., Xue, Q. S., Sankar, V., Nishida, T., Shaw, G., Streit, W. J., and Sanchez, J. C. (2012) Comprehensive characterization and failure modes of tungsten microwire arrays in chronic neural implants. *J. Neural Eng. 9*, 056015.
(49) Lacour, S. P., Courtine, G., and Guck, J. (2016) Materials and technologies for soft implantable neuroprostheses. *Nat. Rev. Mater. 1*, 16063.
(50) Luan, L., Wei, X., Zhao, Z., Siegel, J. J., Potnis, O., Tuppen, C. A., Lin, S., Kazmi, S., Fowler, R. A., Holloway, S., Dunn, A. K., Chitwood, R. A., and Xie, C. (2017) Ultraflexible nanoelectronic probes form reliable, glial scar-free neural integration. *Sci. Adv. 3*, e1601966.
(51) Rivnay, J., Wang, H. L., Fenno, L., Deisseroth, K., and Malliaras, G. G. (2017) Next-generation probes, particles, and proteins for neural interfacing. *Sci. Adv. 3*, e1601649.
(52) Ferro, M. D., and Melosh, N. A. (2018) Electronic and Ionic Materials for Neurointerfaces. *Adv. Funct. Mater. 28*, 1704335.
(53) Salatino, J. W., Ludwig, K. A., Kozai, T. D. Y., and Purcell, E. K. (2017) Glial responses to implanted electrodes in the brain. *Nat. Biomed. Eng. 1*, 862−877.
(54) Gold, C., Henze, D. A., Koch, C., and Buzsaki, G. (2006) On the origin of the extracellular action potential waveform: A modeling study. *J. Neurophysiol. 95*, 3113−3128.
(55) Arenz, A., Silver, R. A., Schaefer, A. T., and Margrie, T. W. (2008) The contribution of single synapses to sensory representation in vivo. *Science 321*, 977−980.
(56) Kodandaramaiah, S. B., Holst, G. L., Wickersham, I. R., Singer, A. C., Franzesi, G. T., McKinnon, M. L., Forest, C. R., and Boyden, E. S. (2016) Assembly and operation of the autopatcher for automated intracellular neural recording in vivo. *Nat. Protoc. 11*, 634−654.
(57) Rios, G., Lubenov, E. V., Chi, D., Roukes, M. L., and Siapas, A. G. (2016) Nanofabricated Neural Probes for Dense 3-D Recordings of Brain Activity. *Nano Lett. 16*, 6857−6862.
(58) Liu, X., McCreery, D. B., Carter, R. R., Bullara, L. A., Yuen, T. G., and Agnew, W. F. (1999) Stability of the interface between neural tissue and chronically implanted intracortical microelectrodes. *IEEE Transactions on Neural Systems and Rehabilitation Engineering 7*, 315−326.
(59) Grady, C. (2012) BRAIN AGEING The cognitive neuroscience of ageing. *Nat. Rev. Neurosci. 13*, 491−505.
(60) Shadlen, M. N., and Newsome, W. T. (1998) The variable discharge of cortical neurons: implications for connectivity, computation, and information coding. *J. Neurosci. 18*, 3870−3896.
(61) Cogan, S. F. (2008) Neural stimulation and recording electrodes. *Annu. Rev. Biomed. Eng. 10*, 275−309.
(62) Kringelbach, M. L., Jenkinson, N., Owen, S. L. F., and Aziz, T. Z. (2007) Translational principles of deep brain stimulation. *Nat. Rev. Neurosci. 8*, 623−635.
(63) Fasano, A., Aquino, C. C., Krauss, J. K., Honey, C. R., and Bloem, B. R. (2015) Axial disability and deep brain stimulation in patients with Parkinson disease. *Nat. Rev. Neurol. 11*, 98−110.
(64) Cicchetti, F., and Barker, R. A. (2014) The glial response to intracerebrally delivered therapies for neurodegenerative disorders: is this a critical issue? *Front. Pharmacol. 5*, 139.
(65) Lin, M. Z., and Schnitzer, M. J. (2016) Genetically encoded indicators of neuronal activity. *Nat. Neurosci. 19*, 1142−1153.
(66) Deisseroth, K. (2015) Optogenetics: 10 years of microbial opsins in neuroscience. *Nat. Neurosci. 18*, 1213−1225.
(67) Calabresi, P., Picconi, B., Tozzi, A., Ghiglieri, V., and Di Filippo, M. (2014) Direct and indirect pathways of basal ganglia: a critical reappraisal. *Nat. Neurosci. 17*, 1022−1030.
(68) Kravitz, A. V., Freeze, B. S., Parker, P. R. L., Kay, K., Thwin, M. T., Deisseroth, K., and Kreitzer, A. C. (2010) Regulation of parkinsonian motor behaviours by optogenetic control of basal ganglia circuitry. *Nature 466*, 622−626.
(69) Zheng, G. F., Patolsky, F., Cui, Y., Wang, W. U., and Lieber, C. M. (2005) Multiplexed electrical detection of cancer markers with nanowire sensor arrays. *Nat. Biotechnol. 23*, 1294−1301.
(70) Gao, N., Zhou, W., Jiang, X., Hong, G., Fu, T.-M., and Lieber, C. M. (2015) General strategy for biodetection in high ionic strength solutions using transistor-based nanoelectronic sensors. *Nano Lett. 15*, 2143−2148.
(71) Fu, T. M., Duan, X. J., Jiang, Z., Dai, X. C., Xie, P., Cheng, Z. G., and Lieber, C. M. (2014) Sub-10-nm intracellular bioelectronic probes from nanowire-nanotube heterostructures. *Proc. Natl. Acad. Sci. U. S. A. 111*, 1259−1264.
(72) Kruskal, P. B., Jiang, Z., Gao, T., and Lieber, C. M. (2015) Beyond the Patch Clamp: Nanotechnologies for Intracellular Recording. *Neuron 86*, 21−24.
(73) Almquist, B. D., and Melosh, N. A. (2010) Fusion of biomimetic stealth probes into lipid bilayer cores. *Proc. Natl. Acad. Sci. U. S. A. 107*, 5815−5820.
(74) Lee, J. H., Zhang, A. Q., You, S. S., and Lieber, C. M. (2016) Spontaneous Internalization of Cell Penetrating Peptide-Modified Nanowires into Primary Neurons. *Nano Lett. 16*, 1509−1513.
(75) Bean, B. P. (2007) The action potential in mammalian central neurons. *Nat. Rev. Neurosci. 8*, 451−465.
(76) Long, M. A., and Lee, A. K. (2012) Intracellular recording in behaving animals. *Curr. Opin. Neurobiol. 22*, 34−44.
(77) Angle, M. R., Cui, B. X., and Melosh, N. A. (2015) Nanotechnology and neurophysiology. *Curr. Opin. Neurobiol. 32*, 132−140.
(78) Whalley, K. (2008) STEM CELLS At home with neural stem cells. *Nat. Rev. Neurosci. 9*, 801−801.
(79) Gao, J., Kim, Y. M., Coe, H., Zern, B., Sheppard, B., and Wang, Y. (2006) A neuroinductive biomaterial based on dopamine. *Proc. Natl. Acad. Sci. U. S. A. 103*, 16681−16686.
(80) Ghashghaei, H. T., Lai, C., and Anton, E. S. (2007) Neuronal migration in the adult brain: are we there yet? *Nat. Rev. Neurosci. 8*, 141−151.

DOI: 10.1021/acs.biochem.8b00122
Biochemistry 2018, 57, 3995−4004